Magnetic Circular Dichroism Spectra of Tris-chelate Complexes of 2,2′-Bipyridyl and 1,10-Phenanthroline with Iron(II), Ruthenium(II), and Osmium(II) at 4.2 K†

Andrew J. Thomson,* Vladimir Skarda, and Michael J. Cook
School of Chemical Sciences, University of East Anglia, Norwich NR4 7TJ
David J. Robbins
Royal Signals and Radar Establishment, St. Andrews Road, Great Malvern, Worcs. WR14 3PS

The magnetic circular dichroism (m.c.d.) spectra, in alcoholic glasses at 4.2 K, are reported for the tris-chelates of 2,2′-bipyridyl and 1,10-phenanthroline of iron(II), ruthenium(II), and osmium(II), including those of the substituted bipyridyl ligands, 4,4′-diphenyl-, 4,4′-diethoxy-, 4,4′-di(ethoxycarbonyl)-, and 5,5′-di(ethoxycarbonyl)-2,2′-bipyridine. The spectra in the region of the spin-allowed metal-to-ligand charge-transfer bands show good resolution and a number of the expected *A*-terms are apparent. The osmium(II) complexes also show well defined *A*-terms in the region of the formally spin-forbidden transitions. Calculation of the signs and magnitudes of the *A*-terms has been carried out using a theoretical model proposed previously. Good agreement is obtained between the experimental results and the theoretical predictions in the case of tris(2,2′-bipyridyl)osmium(II). The relationship between the form of the spectrum of this complex and the others studied is discussed. The m.c.d. spectra of the triplet states do not help to resolve the controversy over the assignment of the luminescing states.

The electronic spectra of the tris-chelates of Fe^{II}, Ru^{II}, and Os^{II} with the ligands 2,2′-bipyridyl (bipy) and 1,10-phenanthroline (phen) have been the subject of a wide range of experimental and theoretical investigations.[1] It was recognised early that the relatively intense absorption bands in the visible region correspond to electronic transitions from orbitals primarily metal in character to orbitals which are ligand-based.[2–8] These metal-to-ligand charge-transfer (c.t.) transitions lead to significant charge separation. This has a number of consquences for the photochemical properties of these complexes.[3] In the case of the Ru^{II} and Os^{II} complexes, photo-luminescence is observed although this is quenched in the Fe^{II} complexes, presumably owing to the presence of *d*-states lying to lower energy of the c.t. transitions.[8]

The assignment of the electronic spectra of these complexes has been difficult and controversial because there appears to be a relatively large number of electronic states arising from the allowed one-electron orbital transitions.[4–8] The complexity of the emitting manifolds of the Ru^{II} and Os^{II} complexes was first demonstrated by Hipps and Crosby[8] in a long series of measurements recording the luminescent quantum efficiencies and decay times at temperatures down to *ca.* 1.6 K. Both of these experimental parameters showed a pronounced change with temperature. A scheme involving three closely spaced levels was proposed to account for the observed behaviour. However, the scheme has recently been called into question.[9]

The intense transitions in the visible region of the spectrum have also proved difficult to assign unambiguously.[10] However, considerable progress has been made recently with the assistance of linear[4–7,11–13] and circular dichroism[12] studies of those complexes doped into crystal lattices at sites of D_3 and C_2 symmetry. This evidence together with a rather detailed theoretical model has arrived at a satisfying assignment.[6]

Magnetic circular dichroism (m.c.d.) spectroscopy has been a useful tool for the assignment of the electronic spectra of transition-metal complexes with axes of at least three-fold rotation symmetry.[14] Hence it might have been expected to play a useful role in assigning the spectra of the D_3 complexes of Fe^{II}, Ru^{II}, and Os^{II}. An early study of the room-temperature m.c.d. spectra of $[Fe^{II}(phen)_3]$ and $[Ru^{II}(phen)_3]$ in solution proved disappointing.[15] The spectra were broad and evidently contained so many overlapping transitions that the m.c.d. terms of the individual transitions could not be resolved. Now we have re-examined the m.c.d. spectra of a variety of D_3 complexes of Fe^{II}, Ru^{II}, and Os^{II} with the ligands bipy and phen, and some of their substituted derivatives. The complexes were dissolved in ethanol–methanol (4:1 v/v) glasses cooled to 4.2 K using a split-coil superconducting magnet. The resulting m.c.d. spectra determined at this temperature are very much better resolved than are the room-temperature spectra and indeed show the expected m.c.d. *A*-terms. The interpretation of the signs of the *A*-terms gives substantial support to the orbital assignments previously suggested both on the basis of theoretical studies and as the result of the polarised crystal spectra.[6]

Experimental

The m.c.d. spectra were measured with a JASCO-J 500D spectropolarimeter fitted with an Oxford Instruments Limited SM4 superconducting solenoid, capable of generating magnetic fields up to 5.3 T. Samples, dissolved in mixtures of ethanol, methanol, and dimethyl sulphoxide, were placed in a 1-mm silica cell and frozen by immersion in liquid helium. The quality of the glass was assessed by measuring the m.c.d. spectra at positive, negative, and zero field. The m.c.d. spectra at positive and negative field formed mirror images of one another, reflected in the zero-field baseline. The absorption spectra of the same samples at liquid helium temperature were recorded in a Cary 17 spectrophotometer.

For calculation of molar absorption coefficients ε (right-hand scale of Figures 1—4) for absorption spectra and Δε (left-hand scale of Figures 1—4) for m.c.d., the concentration of complex ion was taken as 1.25 times the room-temperature value for EtOH–MeOH (4:1 v/v) glass, because of a 20% volume contraction, and as 1.224 times the room-temperature value for EtOH–MeOH–Me_2SO (4:1:1 v/v) glass, because of an 18.3% volume contraction.

† *Non-S.I. unit employed:* B.M. ≃ 9.274 × 10^{-24} J T^{-1}.

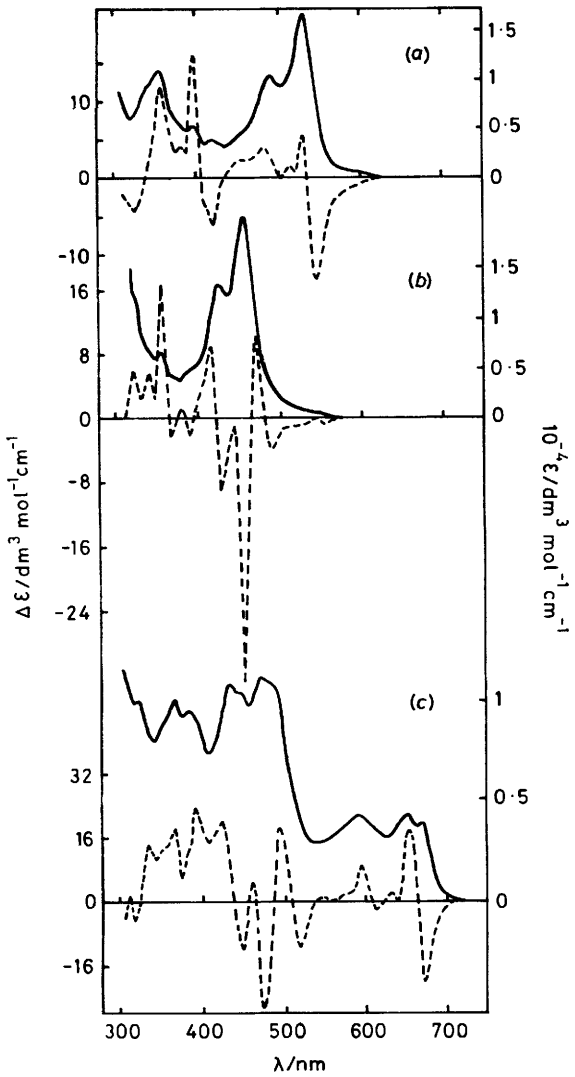

Figure 1. The absorption (———) and m.c.d. spectra (– – – –) (5 T) of (*a*) $[Fe(bipy)_3]^{2+}$, (*b*) $[Ru(bipy)_3]^{2+}$, and (*c*) $[Os(bipy)_3]^{2+}$ in clear EtOH–MeOH (4:1 v/v) glasses at 4.2 K

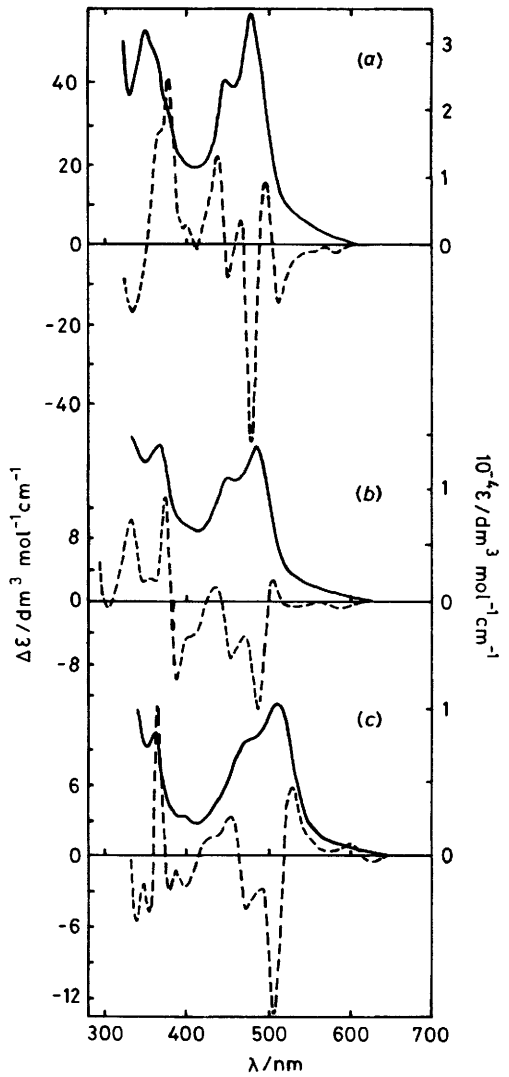

Figure 2. The absorption (———) and m.c.d. spectra (– – – –) (5 T) of (*a*) $[Ru(dpbipy)_3]^{2+}$ in EtOH–MeOH (4:1 v/v) glass; (*b*) $[Ru(debipy)_3]^{2+}$ and (*c*) $[Ru(5,5'\text{-decbipy})_3]^{2+}$ in clear EtOH–MeOH–Me_2SO (4:1:1 v/v) glasses at 4.2 K

Results

The absorption and m.c.d. spectra of the tris-chelated complexes of Fe^{II}, Ru^{II}, and Os^{II} in mixtures of ethanol, methanol, and dimethyl sulphoxide at 4.2 K are shown in Figures 1—4. Figure 1 compares the spectra of the tris-bipy complexes of the three different metal ions and Figure 4 is a comparison of the corresponding tris(phen) complexes. Figure 2 presents the spectra of the tris-chelate complexes of Ru^{II} with the following substituted bipyridyl ligands: 4,4'-diphenyl-2,2'-bipyridine (dpbipy), 4,4'-diethoxy-2,2'-bipyridine (debipy), and 5,5'-di-(ethoxycarbonyl)-2,2'-bipyridine (5,5'-decbipy). Figure 3 gives a comparison of the tris-chelate complexes of Os^{II} with the following substituted ligands: dpbipy, 4,7-diphenyl-1,10-phenanthroline (dpphen), and 4,4'-di(ethoxycarbonyl)-2,2'-bipyridine (4,4'-decbipy). This range of metal ions and ligands was selected in order to provide several series for comparisons to be drawn. First, the effect of the change of the central metal ion is examined. Secondly, the effect of changing the ligand from bipyridyl to phenanthroline can be seen. Finally, some substituted ligands have been selected which give complexes of widely different luminescence quantum efficiencies and lifetimes.[16] For example, $[Ru(dpbipy)_3]^{2+}$ has one of the high quantum efficiencies [0.382 in degassed MeOH–EtOH (4:1 v/v)] and longest lifetimes (1.95 μs) at room temperature known, whereas $[Ru(5,5'\text{-decbipy})_3]^{2+}$ has one of the lowest quantum efficiencies [0.005 in degassed MeOH–EtOH (4:1 v/v)] and shortest lifetime (0.23 μs). The aim was to see whether the m.c.d. spectra could reveal any significant changes in level ordering.

All the spectra show many additional resolved features compared with the room-temperature data. The m.c.d. spectra have sharpened sufficiently to reveal a large number of positive and negative bands and some of the expected *A*-terms are observed. In spite of the obvious complexity there are some features common to the spectra.

The spin-forbidden region of the spectrum at wavelengths longer than 550 nm for the Fe^{II} complexes, longer than 500 nm for the Ru^{II} complexes, and in the range 500—700 nm in the case of the Os^{II} compounds, intensifies rather little in the absorption spectrum from Fe^{II} to Ru^{II} but is very prominent and detailed in the Os^{II} case. The m.c.d. spectra show no discernible features for the Fe^{II} compounds but distinct bands in the case of Ru^{II}.

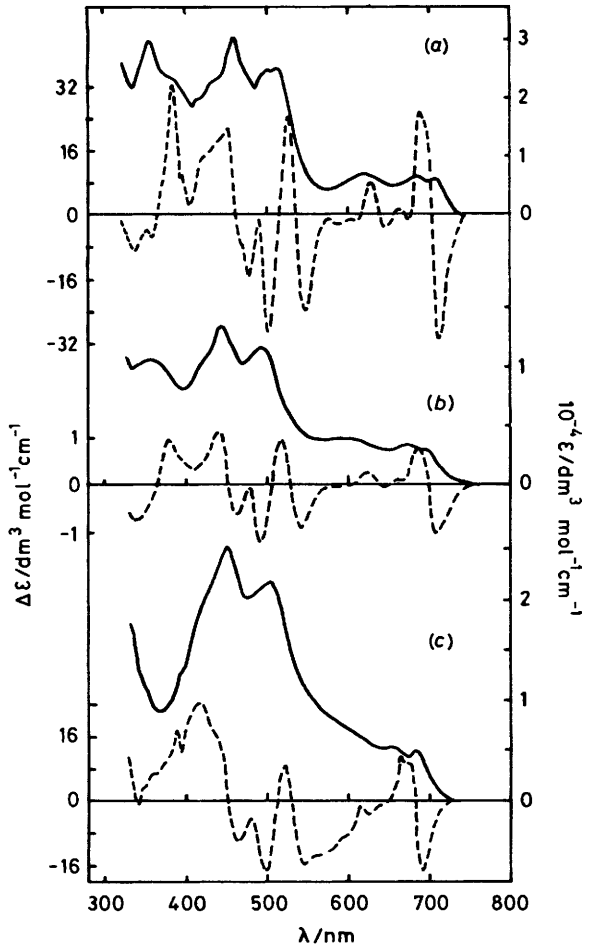

Figure 3. The absorption (———) and m.c.d. spectra (– – – –) (5 T) of (*a*) $[Os(dpbipy)_3]^{2+}$, (*b*) $[Os(4,4'\text{-decbipy})_3]^{2+}$, and (*c*) $[Os(dpphen)_3]^{2+}$ in EtOH–MeOH–Me_2SO (4:1:1 v/v) glasses at 4.2 K

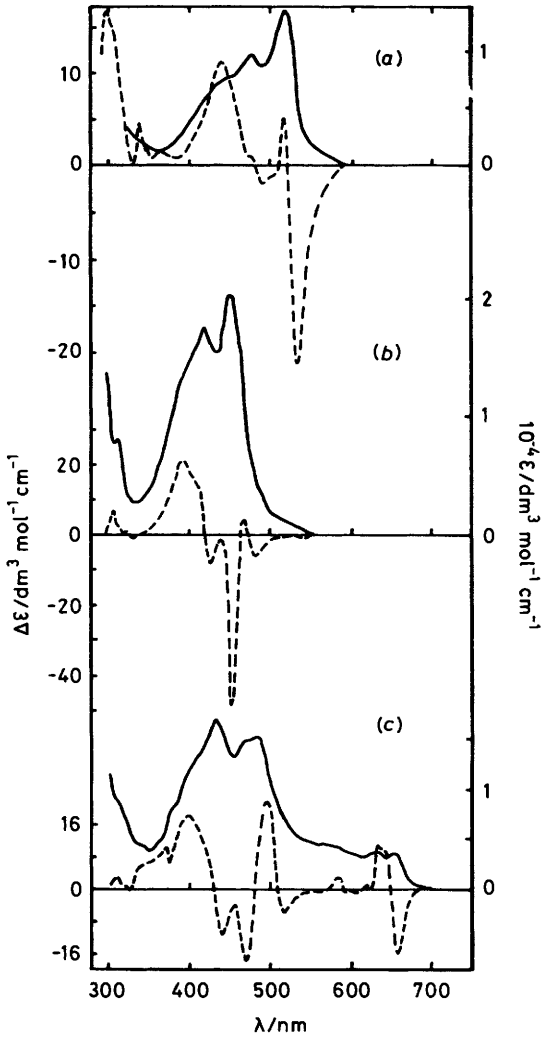

Figure 4. The absorption (———) and m.c.d. spectra (– – – –) (5 T) of (*a*) $[Fe(phen)_3]^{2+}$, (*b*) $[Ru(phen)_3]^{2+}$, and (*c*) $[Os(phen)_3]^{2+}$ in EtOH–MeOH–Me_2SO (4:1:1 v/v) glasses at 4.2 K

However, the m.c.d. spectra of the Os^{II} compounds reveal a number of positive and negative features in the spin-forbidden region. Of note is the fact that the intensity of the m.c.d. spectrum is remarkably constant throughout the spin-forbidden and spin-allowed spectral regions in the case of the Os^{II} complexes although the ε values in the singlet region are about twice those of the triplet. The striking feature is the intense positive *A*-term under the longest wavelength band. This is present in the spectra of all five Os complexes studied here and is followed, at higher energy, by a number of less intense bands which are difficult to analyse in terms of a well-defined *A*-term.

The m.c.d. features in the triplet region of the Ru^{II} complexes are much less clear but, in one case, that of $[Ru(5,5'\text{-decbipy})_3]^{2+}$, Figure 2(*c*), a broad positive *A*-term is detected at *ca.* 620 nm. In all other cases, there appears to be an *A*-term of the same sign superimposed upon a broad negative *B*-term. The m.c.d. spectra of the triplet region of the Fe^{II} complexes are quite devoid of useful features.

When consideration is given to the m.c.d. spectra in the region of the intense c.t. bands it is obvious that the Fe^{II} complexes show a very different pattern to those of Ru^{II} and Os^{II}. We therefore do not consider the Fe^{II} spectra further. However, in the case of the spectra of Ru^{II} and Os^{II} complexes in the range 400—500 nm a very similar pattern of bands is seen. An intense negative trough precedes the main features, then two *A*-terms of opposite sign, negative followed by positive. This pattern of two oppositely signed *A*-terms persists throughout all the Ru^{II} complexes, Figures 1 and 2, and all the Os^{II} complexes, Figures 1 and 3, of the bipyridyl ligands. In the case of two of the Ru^{II} complexes the negative trough is lost, see Figure 2(*b*) and (*c*).

The spectra of the phenanthroline complexes, Figure 4, show some broad similarities to their bipyridyl analogues, Figure 1. The most striking new feature is the rather broad positive band which appears on the short-wavelength side of the visible-region c.t. band.

Theoretical Model

All the metal complexes considered in this paper are diamagnetic, as the temperature independence of the m.c.d. intensity demonstrates, and therefore have the ground-state configuration $t_2{}^6$ under O_h. In the D_3 field of the ligands the t_2 metal orbitals are separated into two sub-sets belonging to the a_1 and *e* representations, Figure 5. The ligand π^* orbitals can be classified as either symmetric (χ) or antisymmetric (ψ) with respect to their two-fold axes.[17] In a trigonal complex possessing three identical ligands the linear combinations of these orbitals lead to pairs of orbitals, a_1 and ε from the χ

Table 1. Metal–ligand c.t. states arising from transitions between $t_{2g}(a_1,e)$ *d*-shell and $\pi^*(a_2,\varepsilon)$ ligand orbitals

Orbital jump	Singlets	Spin–orbit states	Triplets	Spin–orbit states
$a_1 \longrightarrow a_2$	$^1A_2$	$1A_2$	$^3A_2$	$2A_1 + 4E$
$a_1 \longrightarrow \varepsilon$	^1E	$1E$	^3E	$3A_1 + 3A_2 + 5E + 6E$
$e \longrightarrow a_2$	^1E	$2E$	^3E	$4A_1 + 4A_2 + 7E + 8E$
$e \longrightarrow \varepsilon$	^1E	$3E$	^3E	$5A_1 + 5A_2 + 9E + 10E$
	$^1A_1$	$1A_1$	$^3A_1$	$6A_2 + 11E$
	$^1A_2$	$2A_2$	$^3A_2$	$6A_1 + 12E$

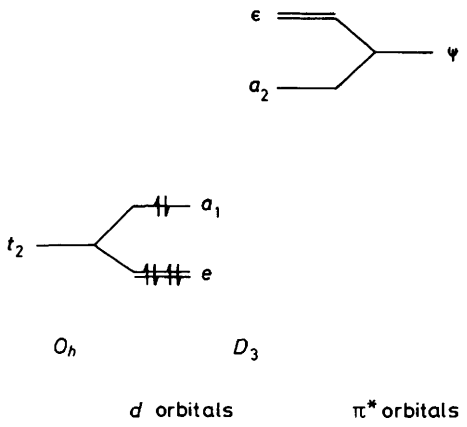

Figure 5. Energy level scheme

Table 2. D_3 basis and state wavefunctions (from ref. 6)

Basis functions ($\omega^{\pm} = e^{\pm 2\pi i/3}$)

$a_1 = 3^{-\frac{1}{2}}(d_{yz} + d_{xz} + d_{xy})$
$e_{\pm} = 3^{-\frac{1}{2}}(\omega^{\pm}d_{yz} + \omega^{\mp}d_{xz} + d_{xy})$
$a_2 = 3^{-\frac{1}{2}}(p + r + q)$
$\varepsilon_{\pm} = \mp 3^{-\frac{1}{2}}(\omega^{\pm}p + \omega^{\mp}r + q)$

State functions

$1A_2$: $2^{-\frac{1}{2}}\{|\bar{a}_1\bar{a}_2\bar{e}_+\bar{e}_+\bar{e}_-\bar{e}_-| - |\bar{a}_1\bar{a}_2\bar{e}_+\bar{e}_+\bar{e}_-\bar{e}_-|\}$

$1E_{\pm}$: $2^{-\frac{1}{2}}\{|\bar{a}_1\bar{\varepsilon}_{\pm}\bar{e}_+\bar{e}_+\bar{e}_-\bar{e}_-| - |\bar{a}_1\bar{\varepsilon}_{\pm}\bar{e}_+\bar{e}_+\bar{e}_-\bar{e}_-|\}$

$2E_+$: $2^{-\frac{1}{2}}\{|\bar{a}_1\bar{a}_1\bar{e}_+\bar{a}_2\bar{e}_-\bar{e}_-| - |\bar{a}_1\bar{a}_1\bar{e}_+\bar{a}_2\bar{e}_-\bar{e}_-|\}$

$2E_-$: $2^{-\frac{1}{2}}\{|\bar{a}_1\bar{a}_1\bar{e}_+\bar{e}_+\bar{e}_-\bar{a}_2| - |\bar{a}_1\bar{a}_1\bar{e}_+\bar{e}_+\bar{e}_-\bar{a}_2|\}$

$3E_+$: $2^{-\frac{1}{2}}\{|\bar{a}_1\bar{a}_1\bar{e}_+\bar{\varepsilon}_-\bar{e}_-\bar{e}_-| - |\bar{a}_1\bar{a}_1\bar{e}_+\bar{\varepsilon}_-\bar{e}_-\bar{e}_-|\}$

$3E_-$: $2^{-\frac{1}{2}}\{|\bar{a}_1\bar{a}_1\bar{e}_+\bar{e}_+\bar{e}_-\bar{\varepsilon}_+| - |\bar{a}_1\bar{a}_1\bar{e}_+\bar{e}_+\bar{e}_-\bar{\varepsilon}_+|\}$

$2A_2$: $2^{-1}\{|\bar{a}_1\bar{a}_1\bar{e}_+\bar{\varepsilon}_+\bar{e}_-\bar{e}_-| - |\bar{a}_1\bar{a}_1\bar{e}_+\bar{\varepsilon}_+\bar{e}_-\bar{e}_-|$
$+ |\bar{a}_1\bar{a}_1\bar{e}_+\bar{e}_+\bar{e}_-\bar{\varepsilon}_-| - |\bar{a}_1\bar{a}_1\bar{e}_+\bar{e}_+\bar{e}_-\bar{\varepsilon}_-|\}$

$2A_1$: $2^{-\frac{1}{2}}\{|\bar{a}_1\bar{a}_2\bar{e}_+\bar{e}_+\bar{e}_-\bar{e}_-| + |\bar{a}_1\bar{a}_2\bar{e}_+\bar{e}_+\bar{e}_-\bar{e}_-|\}$

$4E_{\pm}$: $|\bar{a}_1\bar{a}_2\bar{e}_{\pm}\bar{e}_+\bar{e}_-\bar{e}_-|$

$5E_{\pm}$: $|\bar{a}_1\bar{\varepsilon}_{\pm}\bar{e}_+\bar{e}_+\bar{e}_-\bar{e}_-|$

$8E_+$: $2^{-\frac{1}{2}}\{|\bar{a}_1\bar{a}_1\bar{e}_+\bar{a}_2\bar{e}_-\bar{e}_-| + |\bar{a}_1\bar{a}_1\bar{e}_+\bar{a}_2\bar{e}_-\bar{e}_-|\}$

$8E_-$: $2^{-\frac{1}{2}}\{|\bar{a}_1\bar{a}_1\bar{e}_+\bar{e}_+\bar{e}_-\bar{a}_2| + |\bar{a}_1\bar{a}_1\bar{e}_+\bar{e}_+\bar{e}_-\bar{a}_2|\}$

$9E_+$: $2^{-\frac{1}{2}}\{|\bar{a}_1\bar{a}_1\bar{e}_+\bar{\varepsilon}_-\bar{e}_-\bar{e}_-| - |\bar{a}_1\bar{a}_1\bar{e}_+\bar{\varepsilon}_-\bar{e}_-\bar{e}_-|\}$

$9E_-$: $2^{-\frac{1}{2}}\{|\bar{a}_1\bar{a}_1\bar{e}_+\bar{e}_+\bar{e}_-\bar{\varepsilon}_+| - |\bar{a}_1\bar{a}_1\bar{e}_+\bar{e}_+\bar{e}_-\bar{\varepsilon}_+|\}$

orbitals and a_2 and ε from the ψ orbitals. Considering transitions only to the $\pi^*(\psi)$ orbitals there is a possible total of four one-electron jumps, $a_1 \longrightarrow a_2$, $a_1 \longrightarrow \varepsilon$, $e \longrightarrow a_2$, and $e \longrightarrow \varepsilon$, where ε indicates the doubly degenerate pair of π^* orbitals which transform as *e* under D_3. These four one-electron transitions give rise to 12 states, six spin singlets and six spin triplets, Table 1. (We use throughout the numbering of the states introduced by Ferguson and Herren.[6]) Inclusion of spin–orbit coupling from the metal ion splits the triplet states into 18 spin–orbit components, nine of which are doubly degenerate under D_3. The irreducible representations to which they belong are given in Table 1. The same number of states will arise from the four possible orbital transitions from the metal t_2 *d*-sub-set to the $\pi^*(\chi)$ ligand combination.

The intensities of the allowed charge-transfer transitions have been investigated by Ceulemans and Vanquickenborne[10] (CV model) based upon earlier work of Day and Sanders.[18] The major contribution to the intensity comes from the so-called transfer term which is non-zero only for the transitions $A_1 \longrightarrow E$, corresponding to the orbital transitions $e(t_2) \longrightarrow a_2(\psi^*)$ and $e(t_2) \longrightarrow \varepsilon(\psi^*)$, and also for $e(t_2) \longrightarrow a_1(\chi^*)$ and $e(t_2) \longrightarrow \varepsilon(\chi^*)$. However, the CV model[10] suggested that, for the case of $[Ru(bipy)_3]^{2+}$, both of the transitions to the ψ^* orbitals lie under the broad visible-region absorption band and that the transitions to the χ^* orbitals lie higher in energy.

The transfer-term intensity mechanism leads to transition intensity which is polarised perpendicular (σ) to the C_3 axis of the trigonal complex.[4,7] Thus although group theory allows polarisation parallel to this axis (π-polarisation), there is no intensity in this direction arising from transfer terms. Contributions to the intensity by other mechanisms are possible. For example, 'contact' term intensity is directly proportional to the overlap density of the donor and acceptor orbitals and will lead to weak electric-dipole intensity in all symmetry-allowed metal-to-ligand c.t. bands.[6] Other sources of intensity come from internal metal or ligand transitions, that is, either metal $d \longrightarrow p$ or $\pi \longrightarrow \pi^*$.[6] These latter sources of intensity are important in determining the circular dichroism (c.d.) of these complexes.[12] However, polarised single-crystal experiments on $[Ru(bipy)_3]^{2+}$ in $[Zn(bipy)_3]SO_4{\cdot}7H_2O$,[13] in $[Zn(bipy)_3]Br_2{\cdot}6H_2O$,[4,6] in $[Zn(bipy)_3][BF_4]_2$,[4,6] and in $[Zn(bipy)_3][PF_6]_2$[4,6] have given the polarisation ratios, π/σ, throughout the visible region absorption bands. Similar experiments have been carried out for Os^{2+} and Fe^{2+} in $[Zn(bipy)_3]SO_4{\cdot}7H_2O$ and in $[Zn(bipy)_3][PF_6]_2$.[6,7] These experiments show that the major absorption intensity in the visible region is polarised σ. The spin-forbidden transitions of $[Os(bipy)_3]^{2+}$ also show predominantly σ polarisation. The metal complex in the crystal lattice of $[Zn(bipy)_3][PF_6]_2$ sits at a site of C_2 symmetry. Consequently *E* states are split and give rise to two perpendicularly polarised transitions. Linear dichroism studies of the three metal complexes in this lattice lead to the conclusion that both of the transitions $A_1 \longrightarrow 2E$ and $A_1 \longrightarrow 3E$ lie under the main visible absorption band.[6]

Ferguson and Herren[6] give the matrices of spin–orbit coupling between all the singlet and triplet states (FH model) using the procedure of Sugano *et al.*[19] The metal-ion orbitals were approximated as pure metal *d*-orbitals with no contribution from ligand orbitals. The matrices show (Table 3 of ref. 6) that second-order spin–orbit coupling mixes excited states $2E$ with $4E$ and $8E$ while $3E$ mixes with $5E$ and $9E$. They therefore conclude that only four of the nine *E* triplet states will carry transfer-term intensity, and furthermore, that they will be polarised perpendicular to the molecular C_3 axis.

Our objective in this section is to determine the form of the m.c.d. spectrum for the two singlet transitions $A_1 \longrightarrow 2E$ and $A_1 \longrightarrow 3E$ and for the four triplet transitions $A_1 \longrightarrow 4E$, $8E$

and $A_1 \longrightarrow 5E$, $9E$ which 'borrow' intensity from the two singlet transitions. We calculate the signs and magnitudes of the expected A-terms.

The D_3 basis and state wavefunctions given by Ferguson and Herren[6] have been used throughout. The relevant functions are repeated here for convenience in Table 2. The orbital magnetic moment is non-zero only for the $e_\pm$ d-functions in first order as in equation (1). The orbital moment of the ligand $\varepsilon_\pm$ functions is zero provided that overlap between orbitals on different ligands is ignored.[15]

$$\langle e_\pm|l_z|e_\pm\rangle = \pm 3^{-\frac{1}{2}}\hbar/2\pi \quad (1)$$

Since the major part of absorption intensity is polarised perpendicular to the C_3 axis the definitions (2) and (3) are

$$a_1 = \frac{1}{3}\sum_{\alpha,\lambda}[\langle J\lambda|L_z + 2S_z|J\lambda\rangle - \langle A\alpha|L_z + 2S_z|A\alpha\rangle]\cdot (|\langle A\alpha|m_{-1}|J\lambda\rangle|^2 - |\langle A\alpha|m_{+1}|J\lambda\rangle|^2) \quad (2)$$

$$D_0 = \frac{1}{3}\sum_{\alpha,\lambda}[|\langle A\alpha|m_{+1}|J\lambda\rangle|^2 + |\langle A\alpha|m_{-1}|J\lambda\rangle|^2] \quad (3)$$

required for a transition $A \longrightarrow J$ with electronic components α and λ respectively.[14]

Using standard theory the a_1 and D_0 values for the $A_1 \longrightarrow 2E$ and $A_1 \longrightarrow 3E$ transitions can be readily evaluated. The results are summarised in Table 3. Note that the orbital moment of the $2E$ and $3E$ states arises from the angular momentum of the $e_\pm$ pair of d orbitals. The signs of the A-terms to these two states are opposite as previously pointed out. Since the orbital moments are determined by the d orbitals and not by the ligands the two other allowed singlet transitions, $^1A_1 \longrightarrow {}^1E$, arising from the orbital transitions $a_1(d) \longrightarrow a_1(\chi^*)$ and $e(d) \longrightarrow \varepsilon(\chi^*)$ also have the same signs and magnitudes of A-terms as do $a_1(d) \longrightarrow a_2(\psi^*)$ and $e(d) \longrightarrow \varepsilon(\psi^*)$, respectively. Thus the m.c.d. spectrum provides no distinction between these two assignments.

According to the spin–orbit matrices of the FH model (Table 3 of ref. 6) only four of the 12 triplet states will carry transfer-term intensity. This will be polarised perpendicular to the molecular C_3 axis. Spin–orbit coupling mixes $2E$ with $4E$ and $8E$ while $3E$ mixes with $5E$ and $9E$. Using perturbation theory and the results given in the FH matrices, the perturbed electronic states (designated by primes on the kets) are to lowest order given by equations (4) and (5), where ξ is the spin–orbit

$$|4E_\pm\rangle' = |4E_\pm\rangle + \frac{\xi}{2\varepsilon_1}|2E_\mp\rangle \quad (4)$$

$$|8E_\pm\rangle' = |8E_\pm\rangle + \frac{\xi}{2\varepsilon_2}|8E_\pm\rangle \quad (5)$$

coupling constant of the metal ion, $\varepsilon_1 = W_{2E} - W_{4E}$, and $\varepsilon_2 = W_{2E} - W_{8E}$, the energy gaps between the $2E$ and spin–orbit states, $4E$ and $8E$, respectively.

A similar set of functions, (6) and (7), can be written for the

$$|5E_\pm\rangle' = |5E_\pm\rangle + \frac{(-\xi)}{2\varepsilon_3}|3E_\mp\rangle \quad (6)$$

$$|9E_\pm\rangle' = |9E_\pm\rangle + \frac{(-\xi)}{2\varepsilon_4}|3E_\pm\rangle \quad (7)$$

spin–orbit states $5E$ and $9E$, where $\varepsilon_3 = W_{3E} - W_{5E}$ and $\varepsilon_4 = W_{3E} - W_{9E}$ are the energy separations between the $3E$ and spin–orbit states.

Table 3. Calculated values[a] of a_1 and D_0 for the xy-polarised transition $^1A_1 \longrightarrow S$

S	a_1/m^2 [b]	D_0/m^2 [b]	a_1/D_0 [c]
$2E$ ($e \longrightarrow a_2$)	$-\frac{2}{(3\sqrt{3})}$	$\frac{2}{3}$	$-\frac{1}{\sqrt{3}}$
$4E$ ($a_1 \longrightarrow a_2$)	$-\frac{1}{3}(\xi/\varepsilon_1)^2$	$\frac{1}{6}(\xi/\varepsilon_2)^2$	$+2$
$8E$ ($e \longrightarrow a_2$)	$-\frac{1}{(6\sqrt{3})}(\xi/\varepsilon_2)^2$	$\frac{1}{6}(\xi/\varepsilon_2)^2$	$-\frac{1}{\sqrt{3}}$
$3E$ ($e \longrightarrow \varepsilon$)	$+\frac{2}{(3\sqrt{3})}$	$\frac{2}{3}$	$+\frac{1}{\sqrt{3}}$
$5E$ ($a_1 \longrightarrow \varepsilon$)	$-\frac{1}{3}(\xi/\varepsilon_3)^2$	$\frac{1}{6}(\xi/\varepsilon_3)^2$	-2
$9E$ ($e \longrightarrow \varepsilon$)	$\frac{1}{(6\sqrt{3})}(\xi/\varepsilon_4)^2$	$\frac{1}{6}(\xi/\varepsilon_4)^2$	$+\frac{1}{\sqrt{3}}$

[a] ξ = Spin–orbit coupling constant for metal; ε_n is energy gap between triplet state and singlet state from which electric dipole intensity is 'borrowed'. [b] $m^2 = |\langle 1A_1|m_\pm|S\rangle|^2$. [c] Units are B.M.

Under the point group D_3 a spin triplet, $S = 1$, transforms as $A_2(M_S = 0)$ and $E(M_S = \pm 1)$.[20] Four spin–orbit components, (8)—(11), arise in the following way by coupling the orbital and spin components.

	orbital	spin	
$\|4E_\pm\rangle$	$= \mp i\|A_2\rangle$	$\|E \pm 1\rangle$	(8)
$\|5E_\pm\rangle$	$= \|E \mp 1\rangle$	$\|E \mp 1\rangle$	(9)
$\|8E_\pm\rangle$	$= \mp i\|E \pm 1\rangle$	$\|A_2\rangle$	(10)
$\|9E_\pm\rangle$	$= \mp i\|E \pm 1\rangle$	$\|A_2\rangle$	(11)

Hence, the magnetic moments of these four spin–orbit states divide into two types, either spin-only, (12) and (13), or orbital-only, (15) and (16), because only the $e_\pm$ pair of d orbitals carry

$$\langle 4E_\pm|2S_z|4E_\pm\rangle = \pm 2.0\hbar/2\pi \quad (12)$$

$$\langle 5E_\pm|2S_z|5E_\pm\rangle = \pm 2.0\hbar/2\pi \quad (13)$$

$$\langle 4E_\pm|L_z|4E_\pm\rangle = 0 \text{ and } \langle 5E_\pm|L_z|5E_\pm\rangle = 0 \quad (14)$$

$$\langle 8E_\pm|L_z|8E_\pm\rangle = \pm 3^{-\frac{1}{2}}\hbar/2\pi \quad (15)$$

$$\langle 9E_\pm|L_z|9E_\pm\rangle = \pm 3^{-\frac{1}{2}}\hbar/2\pi \quad (16)$$

$$\langle 8E_\pm|2S_z|8E_\pm\rangle = \langle 9E_\pm|2S_z|9E_\pm\rangle = 0 \quad (17)$$

orbital angular momentum, the ligand orbitals $\varepsilon_{\pm 1}$ having zero to first-order. The g values of these states are $g_\parallel = 4.0$, $g_\perp = 0$ for $4E$ and $5E$ whereas $g_\parallel = 2/\sqrt{3}$, $g_\perp = 0$ for $8E$ and $9E$.[18] The much larger $g_\parallel$ value of the states $4E$ and $5E$ leads to the high values of the A-terms for these excited states.

The Zeeman splitting of the perturbed spin–orbit states is determined by the parent triplet state. However, the electric dipole transition intensity from the $^1A_1$ ground state is governed by a term of the form $(\xi/\varepsilon_n)^2$ in each case since it is the

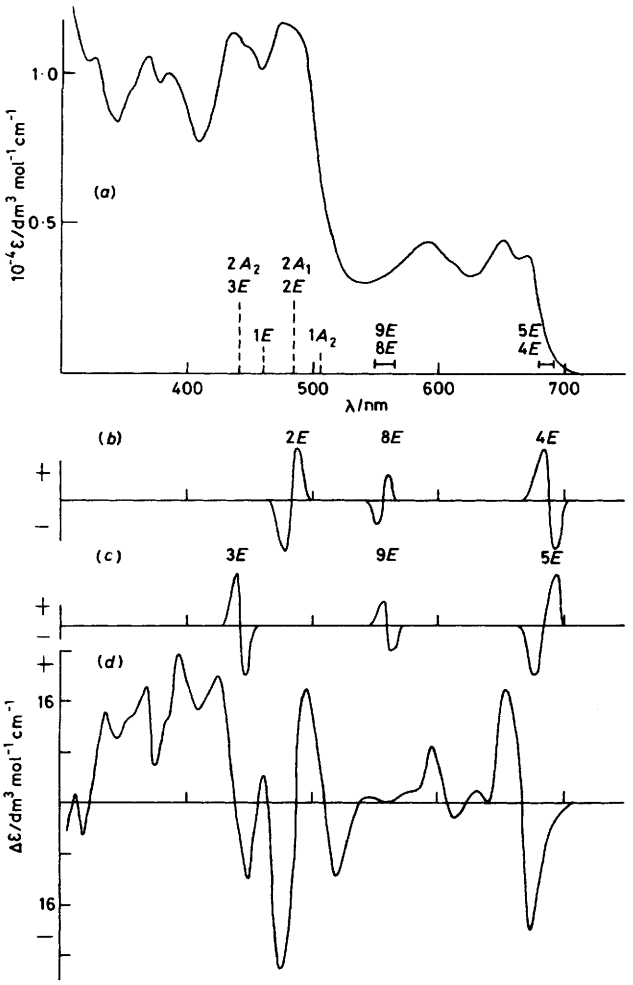

Figure 6. (*a*) Absorption and (*d*) m.c.d. spectra of $[Os(bipy)_3]^{2+}$ in EtOH–MeOH (4:1 v/v) glass at 4.2 K. Vertical dashed lines mark the excited-state energies as calculated by Ferguson and Herren.[11] Spectra (*b*) and (*c*) represent the form of *A*-terms for transitions $^1A_1 \longrightarrow 2E, 4E, 8E$ and $3E, 5E, 9E$, respectively. Shapes and magnitudes are schematic only and not quantitative

two spin-allowed transitions $A_1 \longrightarrow 2E, 3E$ which carry the intensity.

The results evaluated using the expressions given earlier for the a_1 and D_0 terms and the spin–orbit wavefunctions defined above are summarised in Table 3.

A simple pattern is evident from these results. The *A*-terms of the spin–orbit states $4E$ and $5E$ are predicted to be opposite in sign to those of the states $2E$ and $3E$, respectively, from which they 'borrow' electric dipole intensity. On the other hand, the *A*-terms associated with the states $8E$ and $9E$ have the same sign as those of the states with which they mix. Furthermore, because of the larger $g_{\|}$ values of $4E$ and $5E$ compared with $8E$ and $9E$ the former are expected to give the more intense *A*-terms.

The relationship (18) between the theoretical expressions for the *A*-terms and Δε, the experimental differential absorption coefficient, is shown below,[14] where *B* is the magnetic field

$$\frac{\Delta\varepsilon}{\epsilon} = 152.5B\left[a_1\left(-\frac{\delta f}{\delta\epsilon}\right) + B_0 f\right]$$

and

$$\frac{\varepsilon}{\epsilon} = 326.6 D_0 f \qquad (18)$$

intensity in Tesla, ϵ is the energy, B_0 is the *B*-term, D_0 is the dipole strength, and f is a band-shape function.

In Figure 6 we show in schematic form the *A*-terms expected for each of the two allowed transitions $A_1 \longrightarrow 2E$ and $A_1 \longrightarrow 3E$ and their associated spin–orbit partners $4E$, $8E$ and $5E$, $9E$, respectively. The relative energies of the six transitions expected to have transfer-term intensity are taken from the energy calculation of Ferguson and Herren[6] for the case of Os^{2+} doped into $[Zn(bipy)_3][BF_4]_2$. We take this as illustrative at this stage and reserve discussion of the validity of the assignment until later.

The FH energy-level calculation predicts a total of five states, $1A_2$, $2A_2$, $1E$, $2E$, and $3E$ to lie within the intense visible-region absorption bands of both the Ru^{II} and Os^{II} complexes. Hence a number of *B*-terms are likely to arise between these five states and could well have considerable magnitude in view of their close energy spacing. Consideration of the possibilities leads to some interesting simplifications, however. The angular momentum operators L_z and L_x, L_y transform as A_2 and E respectively, under D_3. Therefore there can be non-zero *B*-terms arising from L_z only between *E* states and between A_1 and A_2 states, and in all cases the electric dipole intensity must be *x*,*y* polarised. Inspection of the wavefunctions for these states, Table 2, shows that, if orbital overlap is ignored then the matrix elements of L_z between the five states are all zero. So no *B*-terms are possible for purely *xy*-polarised electric dipole transitions within the approximation of zero overlap. In the case of the *x*,*y* components of the orbital angular momentum operator non-zero matrix elements arise only in the case of $1A_2 \longleftrightarrow 2E$, and are of the form $\langle a_1|l_{\pm}|e_{\mp}\rangle$ where the orbitals a_1 and $e_{\pm}$ correspond to the $M_l = 0, \pm 1$ components of the t_{2g} *d*-orbital sub-set. A further requirement is for the transition to $1A_2$ to have *z*-polarised intensity. It has been pointed out that the 'contact' term will lead to weak electric-dipole intensity in all symmetry-allowed c.t. bands.[6] Another source of intensity for the $^1A_1 \longrightarrow {}^1A_2$ band is the $d \longrightarrow p$ metal-ion transition. Hence our conclusion is that only the $1A_2$ and $2E$ states are likely to have appreciable *B*-term intensity from within the manifold of states thought to be located in the region of the intense c.t. bands.

Assignments and Discussion

Osmium Complexes.—The starting point for our analysis and assignment of the m.c.d. spectra has been the FH energy level calculations.[6] The spectrum of $[Os(bipy)_3]^{2+}$ is the clearest example to analyse. Figure 6 shows the absorption spectrum at 4.2 K with the energies of the important excited states, as calculated by Ferguson and Herren,[11] indicated by dashed lines. In the singlet region only transitions to $2E$ and $3E$ are expected to carry any 'transfer-term' c.t. intensity. The spin-forbidden region should consist of four excited states, namely $4E$, $5E$, $8E$, and $9E$, which borrow electric dipole intensity from the two allowed singlet states. In Figure 6(*b*) and (*c*) are shown the signs of the m.c.d. *A*-terms predicted by the calculations presented in the previous section. Note that the drawing is schematic only and nothing is implied about magnitude by the diagram. The calculated magnitudes are given in Table 4. Figure 6(*d*) shows the experimental m.c.d. spectrum measured at 4.2 K in EtOH—MeOH (4:1 v/v).

Figure 6 shows that the region of the spectrum of 400—500 nm is indeed dominated by two *A*-terms of opposite and absolute signs that agree with the energy assignments of ref. 6. The negative trough in the m.c.d. spectrum at 520 nm lies in the region where the transition to the $1A_2$ state is expected. We showed in the previous section that the transition to this state, although very weak in the absorption spectrum, is expected to give rise to a *B*-term by field-induced mixing with the $2E$ excited

Table 4. Numerical estimates of a_1 and D_0 for Ru^{II} and Os^{II} complexes

	$a_1/m^{2\,a}$	$D_0/m^{2\,a}$	$a_1/D_0{}^b$
Ruthenium(II)			
$2E\,(e \longrightarrow a_2)$	−0.38	0.67	−0.58
$4E\,(a_1 \longrightarrow a_2)$	0.023	0.011	+2.0
$8E\,(e \longrightarrow a_2)$	−0.028	0.048	−0.58
$3E\,(e \longrightarrow \varepsilon)$	0.38	0.67	+0.58
$5E\,(a_1 \longrightarrow \varepsilon)$	−0.011	0.0053	−2.0
$9E\,(e \longrightarrow \varepsilon)$	0.0074	0.013	+0.58
Osmium(II)			
$2E\,(e \longrightarrow a_2)$	−0.38	0.67	−0.58
$4E\,(a_1 \longrightarrow a_2)$	0.09	0.045	+2.0
$8E\,(e \longrightarrow a_2)$	−0.09	0.155	−0.58
$3E\ (e \longrightarrow \varepsilon)$	0.38	0.67	+0.58
$5E\,(a_1 \longrightarrow \varepsilon)$	−0.035	0.018	−2.0
$9E\,(e \longrightarrow \varepsilon)$	0.029	0.051	+0.58

Energy gaps (W/cm^{-1})

For Ru^{II}, ξ = 860 cm^{-1}

$W(2E \longleftrightarrow 4E)$ = 3 300 $W(3E \longleftrightarrow 5E)$ = 4 800

$W(2E \longleftrightarrow 8E)$ = 1 600 $W(3E \longleftrightarrow 9E)$ = 3 100

For Os^{II}, ξ = 2 700 cm^{-1}

$W(2E \longleftrightarrow 4E)$ = 5 200 $W(3E \longleftrightarrow 5E)$ = 8 300

$W(2E \longleftrightarrow 8E)$ = 2 800 $W(3E \longleftrightarrow 9E)$ = 4 900

^{a} $m^2 = |\langle {}^1A_1|M_\pm|{}^1E\rangle|^2$; m^2 is the same for the two orbital transitions $^1E\,(e \rightarrow a_2)$ and $^1E\,(e \rightarrow \varepsilon)$ in the case of ligand acceptor orbitals of ψ type, if the intensity is due only to transfer term. The absolute value of m^2 is different for Ru^{II} and Os^{II}. ^{b} Units are B.M.

state. Since these states are close together according to our assignment then a sizeable B-term is not unexpected. We therefore assign this feature in the m.c.d. spectrum to the $1A_2$ state. The weak positive peak at 460 nm in the m.c.d. spectrum does not appear in the spectra of other Os^{II} complexes, Figure 3. However, a similar feature is apparent in the m.c.d. spectra of $[Ru(dpbipy)_3]^{2+}$, Figure 2. It is possible that this arises from the $1E$ state. However, transitions to this state are not expected to have electric dipole intensity from a 'transfer term'.

In the spin-forbidden region (*ca.* 550—700 nm) of the spectrum of $[Os(bipy)_3]^{2+}$, Figure 6, the most prominent feature is the A-term at 665 nm. This has a positive sign as predicted for the transition to the $4E$ state. However, the FH energy level calculation predicts the $5E$ state to lie virtually degenerate with this state. An estimate can be made of the expected magnitude of the a_1 values for these states, Table 4. By taking a value of 2 700 cm^{-1} for the spin–orbit coupling constant and knowing the energy gap between the $4E$ and $5E$ states and their singlet counterparts $2E$ and $3E$, numerical values (in units of m^2) can be evaluated, Table 4.

The calculations show that the value of a_1 for the $4E$ state is about three times greater than that for the $5E$ state, $0.09m^2$ compared with $-0.035m^2$. The value of a_1/D_0 is calculated to be ± 2.0 B.M. for both states, Tables 3 and 4. A rough estimate of the experimental a_1/D_0 ratio for the A-term at 665 nm in Figure 6 has been obtained by assuming a Gaussian shape for the band. The expressions given by Piepho and Schatz (ref. 14, p. 150), yield a value of +1.0 B.M. We have not attempted detailed fitting or a moments analysis because the corresponding band in the absorption spectrum is not totally resolved but is overlapped by neighbouring peaks. The value of +1.0 B.M. is lower than the predicted value of +2.0 B.M. for a transition only to the $4E$ state. Thus it is possible that the $5E$ state overlaps the $4E$ state and that the corresponding A-term, with opposite sign to that of the $4E$ state, is leading to some cancellation and a lowering of the magnitude of the a_1/D_0 value.

We can therefore conclude only that the m.c.d. spectrum at 660 nm is dominated by the contribution from the $4E$ state and that no direct evidence for the presence of the $5E$ state can be found.

The other region of the m.c.d. spectrum around 600 nm shows complex features that could well arise from the $8E$ and $9E$ states. For example, there appears to be a reasonably intense negative A-term centred at 610 nm which may arise from the $9E$ state. However, without more highly resolved spectra further detailed assignment is only speculative.

The overall pattern observed in the m.c.d. spectrum of $[Os(bipy)_3]^{2+}$ persists, with some variation, in the spectra of the Os^{II} tris-chelate complexes of dpbipy and 4,4′-decbipy, Figure 3. Hence, there has been no significant changes in the level ordering or in the nature of the states. The m.c.d. spectrum of the latter is rather poorly resolved compared with that of the former. Indeed the spectrum of the dpbipy complex has sufficient resolution that the band at 700 nm appears to consist of some structure on the short-wavelength side of the A-term, which may be the transition to the $5E$ state. Also some additional structure is apparent in the short-wavelength region 300—500 nm. We have at present no understanding of the cause of this. It may, however, be related to the degree of excited electron localisation, see later.

Ruthenium Complexes.—The basic pattern for the m.c.d. spectrum of two oppositely signed A-terms under the intense visible-region bands is clearly seen for all the ruthenium complexes reported here, Figures 1 and 2. Again the degree of resolution in the spectra depends upon the substituents on the ligands in a parallel way to that of the osmium compounds. The complex of dpbipy is more highly resolved. In this case a negative m.c.d. band at 515 nm has its counterpart in the spectra of the Os^{II} compounds where we have assigned it to the B-term from the $1A_2$ state. This feature is lost in the less well resolved spectra, Figure 2.

The triplet region of the m.c.d. spectra of the Ru^{II} complexes is poorly resolved and lacks the detail of the spectra of the Os^{II} complexes. Only in the case of the complex of the 5,5′-decbipy, Figure 2, is a broad positive A-term apparent. To this extent there is a parallel with the spectra of the Os^{II} complexes.

Iron(II) Complex.—The m.c.d. spectrum of $[Fe(bipy)_3]^{2+}$ is at first sight markedly different from those of the Ru^{II} and Os^{II} complexes. The negative m.c.d. band assigned to the $1A_2$ state in the spectra of the last two is now one of the dominant features of the spectrum. The remainder of the visible-region spectrum contains no clearly identifiable A-terms. Earlier c.d. work[12] and polarised crystal spectra have assigned a z-polarised band at *ca.* 550 nm in the spectrum of $[Fe(bipy)_3]^{2+}$ to the $1A_2$ state.[5] However the c.d. spectrum of this ion is dominated by two additional sets of bands not observed in the spectra of the Ru^{II} and Os^{II} complexes. It has been suggested that the ligand-field states of Fe^{II} lie within the visible-region c.t. bands and contribute to the c.d. spectrum. It is possible that the m.c.d. spectrum is likewise perturbed from the expected pattern by the presence of these states which should possess orbital angular momentum.

Phenanthroline Complexes.—The m.c.d. and absorption spectra of the 1,10-phenanthroline complexes of Fe^{II}, Ru^{II}, and Os^{II}, Figure 4, show in general an overall similarity to the spectra of the corresponding bipyridyl complexes except that the high-energy side of the c.t. band now has an intense positive

band, visible both in the absorption and m.c.d. spectrum. It is clear that an additional transition has moved down from the near-u.v. region to overlap with the $e \longrightarrow a_2(\psi)$ and $e \longrightarrow \varepsilon(\psi)$ transitions. The calculations of Mayoh and Day[21] predict that the transitions to the χ ligand orbitals will lie at lower energies in the complexes of phenanthroline compared with bipyridyl. Indeed, a comparison of Figures 4 and 1 leads to the conclusion that the spectral features at 300—400 nm in the bipyridyl complexes have moved down to 400 nm in the case of the phen complex of Ru^{II} and Os^{II} and to *ca.* 450 nm in the case of Fe^{II}. There appears in the case of Fe^{II} and Ru^{II} complexes to be a corresponding increase in the negative *B*-term intensity at longer wavelength.

Excited-state Ligand Localisation.—All of the preceding assignment has been carried out under the assumption that the states of the complexes can be classified under the point group D_3. There is no dispute that this is the correct symmetry of the complexes in their electronic ground states. However, there is a good deal of evidence now to suggest that in the excited c.t. state the electron which is transferred to a π^* ligand orbital is localised on one ligand, rather than being delocalised.[22–24] Raman studies of excited-state molecules have shown the presence of vibrations corresponding to $[Ru^{III}(bipy)_2(bipy^-)]^{2+}$.[22,23] For reduced species of these complexes a localisation in the ground state can be observed by e.s.r. spectroscopy.[25] These results raise then the question of the validity of an interpretation of the m.c.d. spectra in terms of a D_3 excited-state geometry.

The answer to this is that there is likely to be only a small effect on the m.c.d. spectrum. We have shown that the *A*-term magnitudes and signs are determined by the orbital angular momentum arising from the *d* shell.[15] No orbital moment can arise in first order from the combination of ligand π^* orbitals even if there is electron delocalisation over all three ligands. If the excited-state symmetry of the complex drops to C_2 then, of course, the orbital degeneracy of the $d_{xz,yz}$ orbitals will be lifted and orbital angular momentum will be quenched to an extent depending upon the magnitude of the C_2 splitting.[6] The consequence for the m.c.d. spectrum will be that the *A*-term, expected under point group D_3, will become two *B*-terms of opposite sign. If the C_2 perturbation leads to a splitting of the excited *E* state which is small compared with the bandwidth of the individual components then an apparent *A*-term will be observed. This will resolve into two *B*-terms only when the C_2 splitting of *E* into *A* and *B* is larger than the bandwidth. Moreover, the first moment of the two *B*-terms will have the same magnitude as that of the *A*-term. In fact, m.c.d. spectra are rather less sensitive to low-symmetry distortions than are the absorption spectra. Thus we conclude that neither the shape nor the magnitude of the m.c.d. spectrum is likely to be changed by a C_2 distortion from D_3. It could be that the splitting of the absorption bands in the spectrum of $[Os(bipy)_3]^{2+}$, Figure 6, at 480 nm and 440 nm into two pairs arises from the lifting of the degeneracy of the $3E(e \longrightarrow \varepsilon)$ and $2E(e \longrightarrow a_2)$ states under the C_2 field caused by excitation localisation. We noted earlier that in the spectra of the three Os^{II} complexes of substituted bipyridyl, Figure 3, the m.c.d. spectra had rather different resolution. This is also seen in the absorption spectra at 4.2 K and the splitting of the pairs of peaks in the visible region follows the order dpbipy > 4,4′-decbipy. We suggest that this corresponds to an order of decreasing ligand localisation or increasing delocalisation of the excited electron.

Acknowledgements

M. J. C. and A. J. T. thank the Ministry of Defence Procurement Executive, D. C. V. D., for funds. We thank Dr. A. P. Lewis and Dr. G. S. G. McAuliffe for assistance in preparing compounds for this work. We thank Professor J. Ferguson (Australian National University, Canberra) for an exchange of views about the spectral assignments proposed in this paper. Results obtained in his laboratory lead him to question some of our conclusions.

References

1 V. Balzani, F. Bolletta, M. T. Gandolfi, and M. Maestri, *Top. Curr. Chem.*, 1978, **75**, 1 and refs. therein.
2 J. P. Paris and W. W. Brandt, *J. Am. Chem. Soc.*, 1959, **81**, 5001.
3 M. Grätzel, K. Kalyanasundarum, and J. Kiwi, *Struct. Bonding (Berlin)*, 1982, **49**, 37.
4 F. Felix, J. Ferguson, H. V. Güdel, and A. Ludi, *J. Am. Chem. Soc.*, 1980, **102**, 4096.
5 F. Felix, J. Ferguson, H. V. Güdel, and A. Ludi, *Chem. Phys. Lett.*, 1979, **62**, 153.
6 J. Ferguson and F. Herren, *Chem. Phys.*, 1983, **76**, 45.
7 S. Decurtins, F. Felix, J. Ferguson, H. V. Güdel, and A. Ludi, *J. Am. Chem. Soc.*, 1980, **102**, 4102.
8 K. W. Hipps and G. A. Crosby, *J. Am. Chem. Soc.*, 1975, **97**, 7042.
9 J. Ferguson and E. R. Krausz, *Chem. Phys. Lett.*, 1982, **93**, 21.
10 A. Ceulemans and L. G. Vanquickenborne, *J. Am. Chem. Soc.*, 1981, **103**, 2238.
11 J. Ferguson and F. Herren, *Chem. Phys. Lett.*, 1982, **89**, 371.
12 J. Ferguson, F. Herren, and G. M. McLaughlin, *Chem. Phys. Lett.*, 1982, **89**, 376.
13 R. A. Palmer and F. S. Piper, *Inorg. Chem.*, 1966, **5**, 864.
14 S. B. Piepho and P. N. Schatz, 'Group Theory in Spectroscopy with Applications to Magnetic Circular Dichroism,' Wiley, New York, 1983.
15 B. R. Hollebone, S. F. Mason, and A. J. Thomson, *Symp. Faraday Soc.*, 1969, **3**, 159.
16 M. J. Cook, A. P. Lewis, G. S. G. McAuliffe, V. Skarda, and A. J. Thomson, *J. Chem. Soc., Perkin Trans. 2*, 1984, 1293.
17 L. E. Orgel, *J. Chem. Soc.*, 1961, 3683.
18 P. Day and N. Sanders, *J. Chem. Soc. A*, 1967, 1530.
19 S. Sugano, Y. Tanabe, and H. Kamimura, 'Multiplets of Transition Metal Ions in Crystals,' Academic Press, New York, 1970, p. 131.
20 G. F. Koster, J. O. Dimmock, R. G. Wheeler, and H. Statz, 'Properties of the Thirty-two Point Groups,' MIT press, Cambridge, Massachussetts, 1963.
21 B. Mayoh and P. Day, *Theor. Chim. Acta*, 1978, **49**, 259.
22 P. G. Bradley, N. Kress, B. A. Hornberger, R. F. Dallinger, and W. H. Woodruff, *J. Am. Chem. Soc.*, 1981, **103**, 7441.
23 R. F. Dallinger and W. H. Woodruff, *J. Am. Chem. Soc.*, 1978, **101**, 4391.
24 M. Forster and R. E. Hester, *Chem. Phys. Lett.*, 1981, **81**, 42.
25 A. G. Motten, K. Hanck, and M. K. DeArmond, *Chem. Phys. Lett.*, 1981, **79**, 541.

Received 6th November 1984; *Paper* 4/1894